ChemComm

COMMUNICATION

View Article Online
View Journal | View Issue

Check for updates

Cite this: *Chem. Commun.*, 2022, **58**, 1534

Received 25th November 2021,
Accepted 29th December 2021

DOI: 10.1039/d1cc06638b

rsc.li/chemcomm

Open Access Article. Published on 30 December 2021. Downloaded on 7/24/2025 3:08:19 PM.
This article is licensed under a Creative Commons Attribution 3.0 Unported Licence.

Acetylene storage performance of [Ni(4,4′-bipyridine)$_2$(NCS)$_2$]$_n$, a switching square lattice coordination network†

Shi-Qiang Wang,[a] Shaza Darwish,[a] Xiao-Qing Meng,[b] Ze Chang,[b] Xian-He Bu[b] and Michael J. Zaworotko*[a]

We report that the previously reported square lattice coordination network [Ni(4,4′-bipyridine)$_2$(NCS)$_2$]$_n$, sql-1-Ni-NCS, undergoes acetylene induced switching between closed (nonporous) and open (porous) phases. The resulting stepped sorption isotherms exhibit temperature controlled steps, consistent high uptake and benchmark working capacity (185 cm^{-3} g^{-1} or 189 cm^{-3}, 1–3.2 bar, 288 K) for acetylene storage.

Acetylene (C_2H_2) is an important chemical feedstock and is also used as a fuel for oxyacetylene torches.[1] However, its highly flammable and explosive nature renders its handling to be more challenging than most gases.[2,3] Current C_2H_2 storage technology involves desensitization by dissolving C_2H_2 in acetone pre-dispersed in a porous monolith that completely fills a gas cylinder.[2,3] The solubility of C_2H_2 in acetone reaches 470.4 cm^{-3} g^{-1} at 15 bar and 288 K.[4] Nevertheless, charging C_2H_2 into acetone dramatically expands the volume of acetone and results in relatively low volumetric uptake (192.3 cm^{-3}).[4] In addition, discharging C_2H_2 releases acetone vapour,[3] precluding its use in production of fine chemicals and electronic materials. Solid sorbents (*e.g.* porous coordination networks, PCNs[5,6]) offer potential to address these handicaps and broaden the utility of C_2H_2 in this "age of gas".[7]

Switching coordination networks (CNs) can be classified as third generation CNs as they can undergo guest-induced structural transformation(s) between "closed" nonporous and "open" porous phases.[8] They represent a small but growing subset of flexible metal–organic frameworks (FMOFs) or soft porous crystals (SPCs).[9–11] Their potential utility is related to their sorption isotherms. Whereas rigid CNs typically exhibit Langmuir (type I) isotherms, switching CNs feature stepped or type F-IV sorption isotherms,[8,12] making them distinctive from most metal–organic materials (MOMs[13,14]) by enhancing working capacity for gas storage (Fig. 1).[8,12,15]

With respect to C_2H_2 storage, a key performance parameter is the working capacity at practically relevant gas delivery (P_{de}) and storage (P_{st}) pressures. We recently proposed that a pressure range of 1–15 bar might be used to define working capacity as this range is compatible with existing C_2H_2–acetone technology.[4] Another important but largely understudied parameter is sorption kinetics, which must be sufficiently fast for

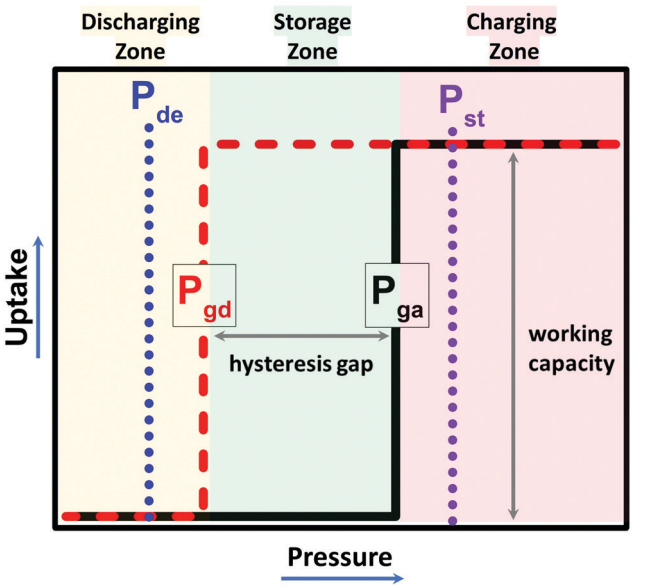

Fig. 1 Schematic illustration of a type F-IV or stepped sorption isotherm. Such isotherms can offer enhanced gas storage performance as, unlike rigid porous materials, working capacity can be 100% of uptake. Black solid line = adsorption branch; red dash line = desorption branch; P_{ga} = gate adsorption pressure; P_{gd} = gate desorption pressure, P_{st} = gas storage pressure; P_{de} = gas delivery pressure.

[a] *Bernal Institute, Department of Chemical Sciences, University of Limerick, Limerick V94 T9PX, Republic of Ireland. E-mail: Michael.Zaworotko@ul.ie*
[b] *School of Materials Science and Engineering, Nankai University, Tianjin 300350, China*

† Electronic supplementary information (ESI) available: Experimental details, desorption isotherms, PXRD patterns, *etc.* See DOI: 10.1039/d1cc06638b

This journal is © The Royal Society of Chemistry 2022

Open Access Article. Published on 30 December 2021. Downloaded on 7/24/2025 3:08:19 PM.
This article is licensed under a Creative Commons Attribution 3.0 Unported Licence.

gas loading and unloading. To date, more than 100 CNs have been investigated with respect to C_2H_2 sorption and most are rigid CNs with high sorption uptake below 1 bar.[16–27] Whereas high uptake can make a sorbent suitable for C_2H_2 sequestration, the type I isotherms typical of rigid sorbents are unlikely to offer a working capacity that is close or equal to their uptake as would be ideal for C_2H_2 storage/delivery.[4] Conversely, switching CNs with a type F-IV isotherm can exhibit a working capacity that equals saturation uptake (Fig. 1). Furthermore, an appropriate hysteresis gap would enable C_2H_2 to be stored at lower pressure (*i.e.* between P_{gd} and P_{ga}) than its charging pressure (*i.e.* P_{ga} and above). A feature of switching CNs is that P_{ga} and P_{gd} can be calculated by applying the Clausius–Clapeyron equation,[4,8] thereby providing an opportunity to calculate C_2H_2 working capacity at higher pressures and avoiding experimental explosion risks. To our knowledge, only two switching CNs, the 3D pillar-layered CN **MOF-508** and the 2D square lattice (**sql**) CN **sql-1-Cu-BF$_4$** (**ELM-11**) have been studied for their C_2H_2 storage properties.[4,19,28] In this contribution, we report that the **sql** CN $[Ni(bpy)_2(NCS)_2]$, **sql-1-Ni-NCS** (1 = bpy = 4,4′-bipyridine) exhibits C_2H_2 induced switching and evaluate its C_2H_2 storage performance by means of variable temperature C_2H_2 sorption studies and *in situ* synchrotron PXRD studies.

sql-1-Ni-NCS was hydrothermally synthesized in 1999 by Zhang *et al.*[29,30] we have developed an alternate route by heating the 1D chain coordination polymer $\{[Ni(bpy)(NCS)_2(H_2O)_2]\cdot bpy\}$ obtained by water slurry.[31] While the crystal structure (Fig. S1, ESI†) and spectroscopic properties of **sql-1-Ni-NCS** are known for two decades,[29,30] its sorption properties were unstudied until we reported its CO_2 sorption properties at low ($\leq$1 bar, 195 K) and high ($\leq$38 bar, 273–298 K) temperatures/pressures.[31] Interestingly, it is the "softest" switching CN with respect to P_{ga} *vs.* its Fe and Co analogues.[31,32] This prompted us to study its C_2H_2 sorption properties since C_2H_2 generally offers stronger sorbent–sorbate interactions than CO_2.[4,8]

The 195 K C_2H_2 sorption isotherm of **sql-1-Ni-NCS** reveals that the P_{ga} is 2.9 kPa (Fig. 2), below the P_{ga} for CO_2 (4.0 kPa).[31] The C_2H_2 uptake plateaus at 185 cm^{-3} g^{-1}, which suggests 4 C_2H_2 molecules per formula unit (**sql-1-Ni-NCS·4C$_2$H$_2$**). This value is 34% higher than the CO_2 saturation uptake (138 cm^{-3} g^{-1}) of **sql-1-Ni-NCS·3CO$_2$**.[31] A second step appeared at *ca.* 60 kPa but does not plateau before 120 kPa. At temperatures above 205 K, the second step was not observed while the initial plateau retained the same saturation uptake. The BET surface area and total pore volume of **sql-1-Ni-NCS** were calculated to be 697.3 m^2 g^{-1} and 0.41 cm^3 g^{-1}, respectively. P_{ga}/P_{gd} values were observed to be 2.9/1.3, 4.1/1.8, 6.8/3.0, 10.2/4.4, 14.9/6.3 and 21.3/9.0 kPa at 195, 199, 205, 210, 215 and 220 K, respectively (Fig. 2 and Fig. S2, ESI†). These temperature and P_{ga}/P_{gd} values were fitted to the Clausius–Clapeyron equation (Fig. 3a and Fig. S3, ESI†), which was used to calculate formation ($\Delta_f H$) and dissociation ($\Delta_d H$) enthalpies (absolute values) of *ca.* 28.5 and 27.7 kJ mol^{-1}, respectively. These ΔH values are comparable to those (28.4/28.2 kJ mol^{-1}) calculated for CO_2 induced phase transition.[31]

P_{ga}/P_{gd} can be calculated at various temperatures once ΔH has been determined.[4,8] We were therefore able to calculate switching pressure *vs* temperature from 195 to 298 K for **sql-1-Ni-NCS** (Fig. 3b and Table S1, ESI†). These plots reveal

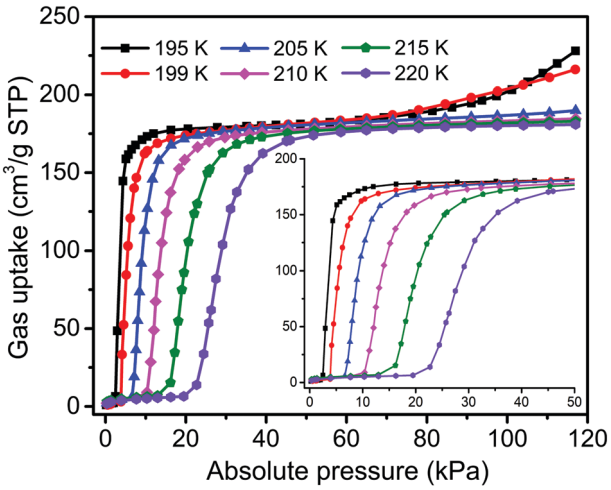

Fig. 2 C_2H_2 (195–220 K) adsorption isotherms for **sql-1-Ni-NCS**.

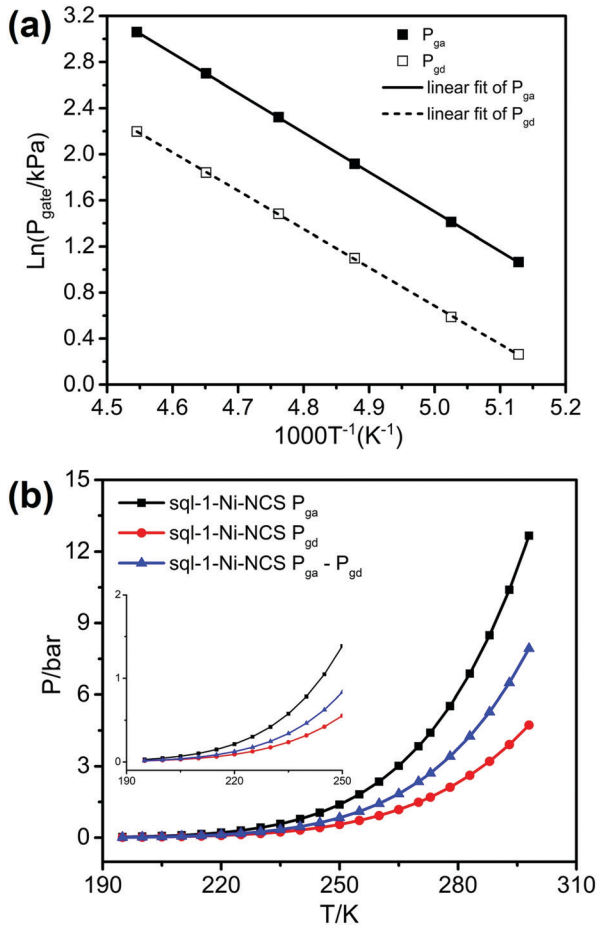

Fig. 3 (a) Linear fit of gate sorption pressure (LnP_{gate}) and temperature (1000/T) using the Clausius–Clapeyron equation; (b) calculated P_{ga}, P_{gd} and the hysteresis gap ($P_{ga} - P_{gd}$) for **sql-1-Ni-NCS**.

Open Access Article. Published on 30 December 2021. Downloaded on 7/24/2025 3:08:19 PM.
This article is licensed under a Creative Commons Attribution 3.0 Unported Licence.

that the C_2H_2 switching pressure and the hysteresis gap between P_{ga} and P_{gd} increase at elevated temperature in a manner similar to that of its CO_2 switching pressures.[31] For example, P_{ga}/P_{gd} were calculated to be 4.4/1.7, 8.5/3.2, and 12.7/4.7 bar at 273, 288, and 298 K, respectively. The corresponding hysteresis gaps were found to be 2.7, 5.3 and 8.0 bar at 273, 288 and 298 K, respectively. These data suggest that C_2H_2 can be stored by **sql-1-Ni-NCS** at lower pressure (*e.g.*, 3.2 bar, 288 K) than the charging pressure (*e.g.*, $\geq$8.5 bar, 288 K).

The related **sql** CN **sql-1-Cu-BF$_4$** was reported to exhibit a type F-IV^m isotherm with three complete C_2H_2 sorption steps at 195 K.[4,8] In contrast, **sql-1-Ni-NCS** exhibited a type F-IV^s isotherm with a single C_2H_2 sorption step. Although the C_2H_2 uptake of **sql-1-Cu-BF$_4$** (245 cm^{-3} g^{-1} at the 3rd plateau) is higher than that of **sql-1-Ni-NCS** (185 cm^{-3} g^{-1} at the 1st plateau), its working capacity is lower between 1–15 bar under ambient temperatures. This is because only the uptake between the second and the third step of **sql-1-Cu-BF$_4$** can be utilised in this pressure range. The working capacity (163 cm^{-3} g^{-1}) of **sql-1-Cu-BF$_4$** is therefore 66.7% of the sorption uptake.[4] In contrast, the uptake of **sql-1-Ni-NCS** can be fully exploited (185 cm^{-3} g^{-1}) under the same conditions so its working capacity is 13.5% above that of **sql-1-Cu-BF$_4$**. With respect to other parameters, the switching pressures (P_{ga}/P_{gd}) and hysteresis gaps are comparable (Fig. S4 and S5, ESI†): P_{gd} values for **sql-1-Ni-NCS** are slightly (0.01–0.34 bar) lower than $P_{gd}3$ of **sql-1-Cu-BF$_4$** in the range 195–298 K; P_{ga} values are 0.04–0.40 bar lower between 195–278 K and 0.08–1.31 bar higher between 283–298 K than those ($P_{ga}3$) of **sql-1-Cu-BF$_4$**. For example, at 288 K, the P_{ga}/P_{gd} values are 8.1/3.5 and 8.5/3.2 bar for **sql-1-Cu-BF$_4$** and **sql-1-Ni-NCS**, respectively.

To gain insight into the nature of the phase transformation induced by C_2H_2, *in situ* synchrotron PXRD experiments were conducted. As shown in Fig. 4a, the phase transformation was complete within 8 min under 0.5 bar C_2H_2 at 195 K. Such sorption kinetics are adequate for practical utility and comparable with the CO_2 sorption kinetics.[31] From a structural perspective, synchrotron PXRD refinement revealed that the unit-cell parameters of **sql-1-Ni-NCS·4C$_2$H$_2$** differ from those of **sql-1-Ni-NCS·3CO$_2$** (Fig. 4b, Fig. S6 and S7, ESI†). For instance, **sql-1-Ni-NCS·3CO$_2$** retained the same space group, *C*2/*c*, as the closed phase of **sql-1-Ni-NCS**, while **sql-1-Ni-NCS·4C$_2$H$_2$** adopted space group *P*2$_1$/*n* as did the *m*-xylene loaded phase (**sql-1-Co-NCS·4MX**) previously reported by us.[33] The Z value is 4 in the closed phase and 2 in the C_2H_2-loaded phase. The normalized unit-cell volume changes from 2264.9 Å^3 in the closed phase to 3181.8 (*i.e.*, 1590.9 × 2) Å^3 in the C_2H_2-loaded phase, correspond to a 40.5% increase in unit cell volume. Attempts to solve the crystal structure of **sql-1-Ni-NCS·4C$_2$H$_2$** were unsuccessful, but MX molecules reside in both interlayer spaces and square cavities in **sql-1-Co-NCS·4MX** (Fig. S8, ESI†).

Volumetric working capacity for gas storage is also a key performance parameter since container volume is necessarily limited. The network density (excluding C_2H_2) of **sql-1-Ni-NCS·4C$_2$H$_2$** was calculated to be 1.02 g cm^{-1} (Fig. 4b), and therefore the volumetric working capacity of C_2H_2 is *ca.* 189 cm^{-3}.

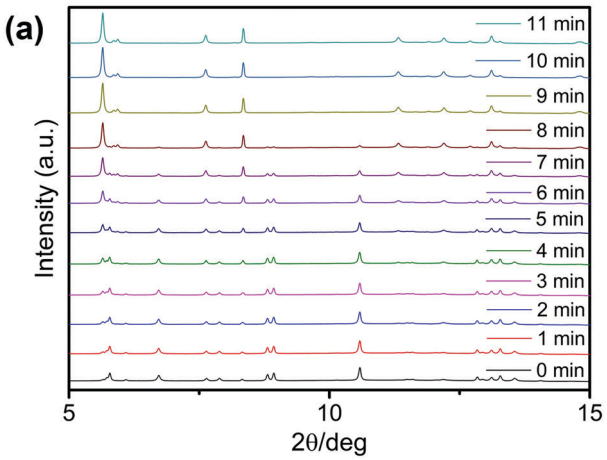

(b)

	Closed	3CO$_2$	4C$_2$H$_2$	4MX
SG	C2/c	C2/c	P2$_1$/n	P2$_1$/n
a/Å	12.156	12.601	10.118	11.394
b/Å	11.381	11.368	16.117	16.103
c/Å	16.646	19.563	10.065	13.328
β/º	100.43	93.41	104.21	97.91
V/Å^3	2264.9	2797.3	1590.9	2422.0
Z	4	4	2	2
D$_{net}$/g cm^{-3}	1.43	1.16	1.02	0.67

Fig. 4 (a) *In situ* synchrotron PXRD patterns for **sql-1-Ni-NCS** under 0.5 bar C_2H_2 at 195 K; (b) structural parameters of **sql-1-Ni-NCS** (closed), **sql-1-Ni-NCS·3CO$_2$**, **sql-1-Ni-NCS·4C$_2$H$_2$** and **sql-1-*Co*-NCS·4MX**.

This value is higher than **sql-1-Cu-BF$_4$** (174 cm^{-3}) and **MOF-508** (106 cm^{-3}).[4,28] When compared to the industrial adsorbent acetone, which has a volumetric working capacity (170 cm^{-3}) between 1–15 bar at 288 K,[4] **sql-1-Ni-NCS** outperforms it by 11.2% at a safer working pressure range (1–3.2 bar, 288 K).

In summary, we herein report a switching transformation in a 2D **sql** CN, **sql-1-Ni-NCS**, induced through exposure to C_2H_2. The C_2H_2 switching pressure, P_{ga}/P_{gd}, was controlled by temperature with retention of the saturation uptake. The type F-IV isotherm exhibited by **sql-1-Ni-NCS** enabled working capacity to be 100% of uptake capacity and the relatively high density resulted in benchmark volumetric working capacity at practically relevant conditions. When combined with other features such as fast sorption kinetics, hydrophobicity, and ease of scale-up,[31] **sql-1-Ni-NCS** is a promising candidate for enhancing the working capacity of gas storage and highlights the general potential that layered CNs offer for high working capacity. This is perhaps counterintuitive since such CNs are nonporous in their closed phases. Further studies to explore the storage potential of **sql-1-Ni-NCS** and related switching adsorbent layered materials (SALMAs) for other gases and vapours are in progress.

M. J. Z. gratefully acknowledges the support of the Irish Research Council (IRCLA/2019/167) and Science Foundation

 This journal is © The Royal Society of Chemistry 2022

Ireland (16/IA/4624). Z. C. and X.-H. B. acknowledge the National Science Foundation of China (NSFC) (21531005) and the Programme of Introducing Talents of Discipline to Universities (B18030). We thank Dr Claire Murray and Dr Chiu C. Tang at the Diamond Light Source, UK, for providing access to the synchrotron X-ray diffraction beamline i11 (EE20500). S.-Q. W. would also like to thank his colleagues, Mr Daniel O'Hearn, Dr Andrey Bezrukov and Dr Soumya Mukherjee, for their assistance at Diamond Light Source.

Open Access Article. Published on 30 December 2021. Downloaded on 7/24/2025 3:08:19 PM.
This article is licensed under a Creative Commons Attribution 3.0 Unported Licence.

Conflicts of interest

There are no conflicts to declare.

Notes and references

1 H. J. Arpe, *Acetylene. Industrial Organic Chemistry*, Wiley, 5th edn, 2010, pp 91–105.
2 R. E. Gannon, R. M. Manyik, C. Dietz, H. Sargent, R. Thribolet and R. Schaffer, Acetylene, *Kirk-Othmer Encyclopedia of Chemical Technology*, Wiley, 2003.
3 P. Pässler, W. Hefner, K. Buckl, H. Meinass, A. Meiswinkel, H.-J. Wernicke, G. Ebersberg, R. Müller, J. Bässler, H. Behringer and D. Mayer, Acetylene, *Ullmann's Encyclopedia of Industrial Chemistry*, Wiley-VCH, 2011.
4 S.-Q. Wang, X.-Q. Meng, M. Vandichel, S. Darwish, Z. Chang, X.-H. Bu and M. J. Zaworotko, *ACS Appl. Mater. Interfaces*, 2021, **13**, 23877–23883.
5 C. Janiak and J. K. Vieth, *New J. Chem.*, 2010, **34**, 2366–2388.
6 D. J. O'Hearn, A. Bajpai and M. J. Zaworotko, *Small*, 2021, 2006351.
7 S. Kitagawa, *Angew. Chem., Int. Ed.*, 2015, **54**, 10686–10687.
8 S.-Q. Wang, S. Mukherjee and M. J. Zaworotko, *Faraday Discuss.*, 2021, **231**, 9–50.
9 A. Schneemann, V. Bon, I. Schwedler, I. Senkovska, S. Kaskel and R. A. Fischer, *Chem. Soc. Rev.*, 2014, **43**, 6062–6096.
10 Z. Chang, D.-H. Yang, J. Xu, T.-L. Hu and X.-H. Bu, *Adv. Mater.*, 2015, **27**, 5432–5441.
11 S. Horike, S. Shimomura and S. Kitagawa, *Nat. Chem.*, 2009, **1**, 695–704.
12 Q. Y. Yang, P. Lama, S. Sen, M. Lusi, K. J. Chen, W. Y. Gao, M. Shivanna, T. Pham, N. Hosono, S. Kusaka, J. J. Perry IV, S. Ma, B. Space, L. J. Barbour, S. Kitagawa and M. J. Zaworotko, *Angew. Chem., Int. Ed.*, 2018, **57**, 5684–5689.
13 J. J. Perry IV, J. A. Perman and M. J. Zaworotko, *Chem. Soc. Rev.*, 2009, **38**, 1400–1417.
14 T. R. Cook, Y.-R. Zheng and P. J. Stang, *Chem. Rev.*, 2012, **113**, 734–777.
15 J. A. Mason, J. Oktawiec, M. K. Taylor, M. R. Hudson, J. Rodriguez, J. E. Bachman, M. I. Gonzalez, A. Cervellino, A. Guagliardi, C. M. Brown, P. L. Llewellyn, N. Masciocchi and J. R. Long, *Nature*, 2015, **527**, 357–361.
16 R. Matsuda, R. Kitaura, S. Kitagawa, Y. Kubota, R. V. Belosludov, T. C. Kobayashi, H. Sakamoto, T. Chiba, M. Takata, Y. Kawazoe and Y. Mita, *Nature*, 2005, **436**, 238–241.
17 D. G. Samsonenko, H. Kim, Y. Sun, G.-H. Kim, H.-S. Lee and K. Kim, *Chem. – Asian J.*, 2007, **2**, 484–488.
18 D. Tanaka, M. Higuchi, S. Horike, R. Matsuda, Y. Kinoshita, N. Yanai and S. Kitagawa, *Chem. – Asian J.*, 2008, **3**, 1343–1349.
19 S. Xiang, W. Zhou, J. M. Gallegos, Y. Liu and B. Chen, *J. Am. Chem. Soc.*, 2009, **131**, 12415–12419.
20 J.-P. Zhang and X.-M. Chen, *J. Am. Chem. Soc.*, 2009, **131**, 5516–5521.
21 S. Xiang, W. Zhou, Z. Zhang, M. A. Green, Y. Liu and B. Chen, *Angew. Chem., Int. Ed.*, 2010, **49**, 4615–4618.
22 Z. Zhang, S. Xiang and B. Chen, *CrystEngComm*, 2011, **13**, 5983–5992.
23 J. Pang, F. Jiang, M. Wu, C. Liu, K. Su, W. Lu, D. Yuan and M. Hong, *Nat. Commun.*, 2015, **6**, 7575.
24 S. Gao, C. G. Morris, Z. Lu, Y. Yan, H. G. W. Godfrey, C. Murray, C. C. Tang, K. M. Thomas, S. Yang and M. Schroder, *Chem. Mater.*, 2016, **28**, 2331–2340.
25 F. Moreau, I. da Silva, N. H. Al Smail, T. L. Easun, M. Savage, H. G. W. Godfrey, S. F. Parker, P. Manuel, S. Yang and M. Schröder, *Nat. Commun.*, 2017, **8**, 14085.
26 Y. He, F. Chen, B. Li, G. Qian, W. Zhou and B. Chen, *Coord. Chem. Rev.*, 2018, **373**, 167–198.
27 Y.-P. Li, Y. Wang, Y.-Y. Xue, H.-P. Li, Q.-G. Zhai, S.-N. Li, Y.-C. Jiang, M.-C. Hu and X. Bu, *Angew. Chem., Int. Ed.*, 2019, **58**, 13590–13595.
28 M. Bonneau, C. Lavenn, K. Sugimoto, A. Legrand, T. Ogawa, F.-X. Coudert, R. Réau, K.-i. Otake and S. Kitagawa, *Res. Square*, 2020, DOI: 10.21203/rs.3.rs-102861/v1.
29 Z. Yugen, J. Li, W. Deng, N. Masayoshi and I. Tsuneo, *Chem. Lett.*, 1999, 195–196.
30 Y. Zhang, L. Jianmin, M. Nishiura and T. Imamoto, *J. Mol. Struct.*, 2000, **519**, 219–224.
31 S.-Q. Wang, S. Darwish, D. Sensharma and M. J. Zaworotko, *Mater. Adv.*, 2022, **3**, DOI: 10.1039/D1MA00785H, accepted.
32 S.-Q. Wang, Q.-Y. Yang, S. Mukherjee, D. O'Nolan, E. Patyk-Kazmierczak, K.-J. Chen, M. Shivanna, C. Murray, C. C. Tang and M. J. Zaworotko, *Chem. Commun.*, 2018, **54**, 7042–7045.
33 S.-Q. Wang, S. Mukherjee, E. Patyk-Kaźmierczak, S. Darwish, A. Bajpai, Q.-Y. Yang and M. J. Zaworotko, *Angew. Chem., Int. Ed.*, 2019, **58**, 6630–6634.